# Hollow Microspherical Architectures of Closely Packed and Radially Well-Aligned $Zn_2SiO_4$ Nanowires with and without ZnO Nanocrust

**Qing Wei, Guowen Meng,* Min Ye, Xiaohong An, Yufeng Hao, and Lide Zhang**

*Key Laboratory of Materials Physics, Anhui Key Laboratory of Nanomaterials and Nanostructures, Institute of Solid State Physics, Chinese Academy of Sciences, Hefei 230031, People's Republic of China*

*Received: October 11, 2006; In Final Form: November 20, 2006*

Microscale hollow spherical architectures consisting of closely packed and radially well-aligned $Zn_2SiO_4$ nanowires (NWs) with and without ZnO spherical nanocrust have been achieved on Si wafers through a simple thermal evaporation and condensation process by using a mixture of any of three carbonates ($ZnCO_3$·$2Zn(OH)_2$·$H_2O$, $(MgCO_3)_4$·$Mg(OH)_2$·$5H_2O$, and $MnCO_3$) and graphite at the bottom and a layer of zinc powder on top as source materials. The major hollow spherical architectures consist of closely packed and well-aligned $Zn_2SiO_4$ NWs growing radially inward from the inner surface of ZnO outer nanocrust. The minor ones are composed of oriented $Zn_2SiO_4$ NWs growing radially outward, with the NW tips forming numerous architectures looking like Chinese writing brush heads. The ZnO outer nanocrust has a strong UV emission at about 390 nm and a green one at about 510 nm, while the well-aligned $Zn_2SiO_4$ NWs have a broad green emission centered at about 520 nm. The novel hollow spherical architectures may have potentials in future nanotechnology.

## 1. Introduction

With ongoing nanotechnology, much attention has been paid to assembling individual one- and two-dimensional (1D and 2D) nanostructures, with controlled size, morphology, chemical composition, crystal phase, and growth orientation into integrated functional nano- and microarchitectures for future device applications.[1] Hollow architectures have potential applications in many fields, such as catalysts, fillers, microreactors,[2] superhydrophilic surfaces,[3] controlled release capsules, artificial cells, chemical sensors, and adsorbents.[4] Thus, organizing 1D or 2D nanostructures into hollow spherical architectures represents one of the challenges for the assembly of individual nanostructures.[5,6] For example, urchinlike architectures of ZnO nanowires (NWs) on external surface of ZnO hollow spheres[7] and mesoporous shells formed by textured ZnO nanocrystals[8] have been fabricated by using a vapor evaporation and deposition process. Meanwhile, dandelion-like architectures of ZnO[9] and CuO,[5] microscale hemispheres and spheres consisting of ZnO nanorods and nanosheets,[10] mesoscopic hollow structures composed of metal−polymer rods,[11] and nanourchin composed of $VO_x$ nanotubes[12] have been achieved through solution methods. Most of the reported composite architectures are composed of binary compound nanomaterials. However, little has been reported on the assembly of ternary compound nanostructures, especially silicate NWs, into hollow spherical architectures. On the other hand, as for the reported composite hollow architectures, the building blocks of 1D NWs, nanorods, or 2D nanosheets usually grow on the external surface of the spherical crust of the same material[7,12] or directly form themselves into spherical shells.[5,8−11] Nothing has been reported on the fabrication of composite hollow spherical architectures consisting of radially well-aligned NWs of one material growing on the inner surface of spherical nanoscale crust of other materials with different properties.

Zinc oxide (ZnO), an important material with semiconductivity and piezoelectric and pyroelectric properties,[13] has potential applications in electronic and optoelectronic devices and in electromechanically coupled sensors and transducers.[14] Especially, ZnO is a crucial photoluminescence material and can achieve effecient excitonic laser action at room temperature because of its wide band gap (3.37 eV) with a large exciton binding energy (60 meV).[14] Zinc silicate ($Zn_2SiO_4$), especially doped with transition or rare earth ions, is a green luminescence material widely used in phosphor hosts, plasma display panels,[15] cathode ray tubes,[15] and fluorescent lamps.[16] It therefore can be expected that if two nanostructured materials with different photoluminescence properties, such as ZnO spherical nanocrusts and $Zn_2SiO_4$ NWs, can be assembled into composite structures, the unique architectures would have potential applications in future optoelectronic nanodevices.

Here, we report the synthesis of two types of microscale hollow spherical architectures, consisting of closely packed and radially well-aligned $Zn_2SiO_4$ NWs with and without a thin spherical outer crust of ZnO, by a thermal evaporation and condensation process without using any catalysts. For type I hollow spherical architectures, the closely packed and well-aligned $Zn_2SiO_4$ NWs grow radially inward on the inner surface of a thin spherical outer crust of ZnO. As for type II hollow spherical architectures, bundles of highly oriented $Zn_2SiO_4$ NWs grow radially outward, directly forming themselves into the spherical shells, with the NW tips forming numerous architectures looking like Chinese writing brush heads. It is striking to find out that when any one of three different carbonates ($ZnCO_3$·$2Zn(OH)_2$·$H_2O$, $(MgCO_3)_4$·$Mg(OH)_2$·$5H_2O$, and $MnCO_3$) was used in the mixture as the raw materials, the final products have similar morphologies and chemical compositions, providing a general approach to the hollow spherical architectures. Photoluminescence measurements reveal that the aligned $Zn_2SiO_4$ NWs have a green emission at about 520 nm, while the spherical

* To whom correspondence should be addressed. E-mail: gwmeng@issp.ac.cn.

10.1021/jp0666737 CCC: $37.00 
Published on Web 01/12/2007

outer crust of ZnO has a strong ultraviolet emission at about 390 nm and a broad green emission centered at about 510 nm.

## 2. Experimental Section

A mixture of $ZnCO_3 \cdot 2Zn(OH)_2 \cdot H_2O$ and graphite in a molar ratio of 2:1 was loaded in a ceramic boat. A thin layer of Zn powder (0.65 g) was placed on the mixture. The ceramic boat with the raw materials was positioned in the hot zone of a horizontal electronic resistance furnace with an alumina tube mounted inside. An ultrasonically cleaned n-type (100) Si substrate was placed downstream about 8 cm from the source materials. High-purity Ar flew through the tube during the experiment at a rate of 20 sccm (standard cubic centimeters per minute). First, the tube furnace was heated to 450 °C from room temperature at a heating rate of 100 °C/min and was kept at this temperature for 5 min. Then, the furnace was heated to 1000 °C from 450 °C in 6 min and was maintained at 1000 °C for 2 h. In the end, the system was naturally cooled down to room temperature. In addition, we substituted $(MgCO_3)_4 \cdot Mg(OH)_2 \cdot 5H_2O$ and $MnCO_3$ for $ZnCO_3 \cdot 2Zn(OH)_2 \cdot H_2O$ in the source materials with other experimental parameters being identical. Although different carbonates were used in the source materials, the same hoar raised products were found on the Si wafers, and it is striking to find out that the final products have similar morphologies and chemical compositions. The as-synthesized products were characterized by using scanning electron microscopy (SEM, Sirion 200), transmission electron microscopy (TEM, Hitachi 800 at 200kv), high-resolution TEM (HRTEM, JEOL 2010 at 200 kV), and energy-dispersive X-ray spectroscopy (EDS) attached to TEM instruments. Room-temperature photoluminescence (PL) spectra were recorded on a LabRam-HR microRaman spectrometer (Jobin-Yvon).

## 3. Results and Discussions

Now, we discuss the morphology and structure of the hollow microspherical architecture obtained by using three kinds of carbonates.

**3.1. Hollow Microspherical Architectures Obtained by Using $ZnCO_3 \cdot 2Zn(OH)_2 \cdot H_2O$ in the Raw Materials.** Low-magnification SEM observation (Figure 1a) of the final products, obtained using $ZnCO_3 \cdot 2Zn(OH)_2 \cdot H_2O$ in the mixture, shows that the Si wafer is covered with spherical architectures with diameters about several hundreds of micrometers. Detailed SEM observations reveal that there exist two types of spherical architectures. The major ones have a smooth-faced outer surface (named type I). Statistic counting of 20 spheres on the Si wafer shows that 80% of the spheres belong to type I. The inset in Figure 1b is a typical broken sphere of type I. An enlarged SEM image (Figure 1b) taken from the broken area indicates that the sphere is not solid but hollow. The shell consists of closely packed and radially well-aligned NWs growing inward from the inner surface of a spherical outer nanocrust. Figure 1c clearly depicts a side view of the spherical shell. A close-up view of the NW tips (the inner surface of the hollow sphere) is displayed on the upper-right corner, demonstrating that the NWs on the inner surface of the spherical outer crust are well-aligned and closely packed. A close-up view of the NWs near the inner surface of the spherical outer crust is inserted on the lower-left corner, clearly indicating that the closely packed NWs grow from the inner surface of the outer spherical crust with a thickness of about 100 nm.

The minor spheres (about 20% in population), named type II, are presented in Figure 2. A typical SEM image (Figure 2a) reveals that the outer surface of type II hollow sphere is not

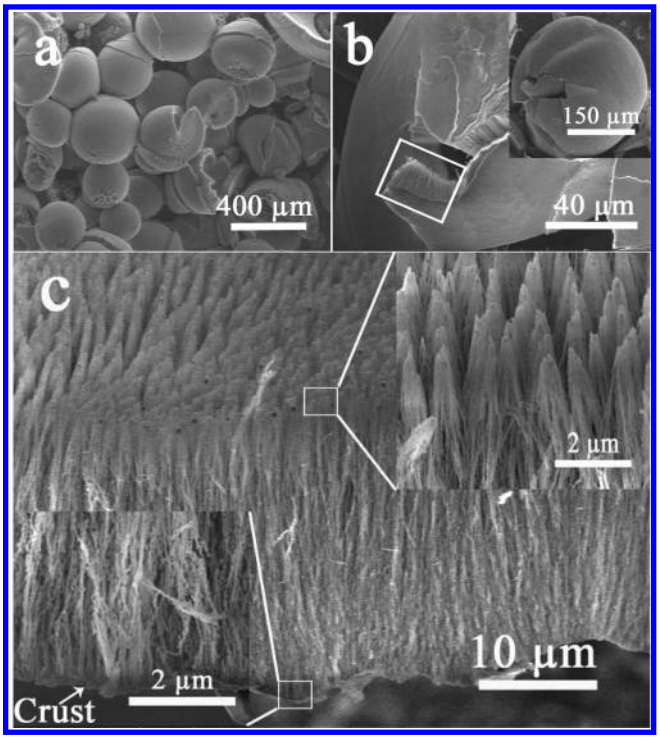


**Figure 1.** (a) Low-magnification SEM image of the spherical architectures on the Si wafer, achieved by using zinc hydroxide carbonate in the mixture and by heating at 1000 °C for 2 h. (b) Enlarged SEM image from the broken area of a type I hollow sphere (the inset). (c) A side view high-magnification SEM image of the "shell" of the hollow sphere.

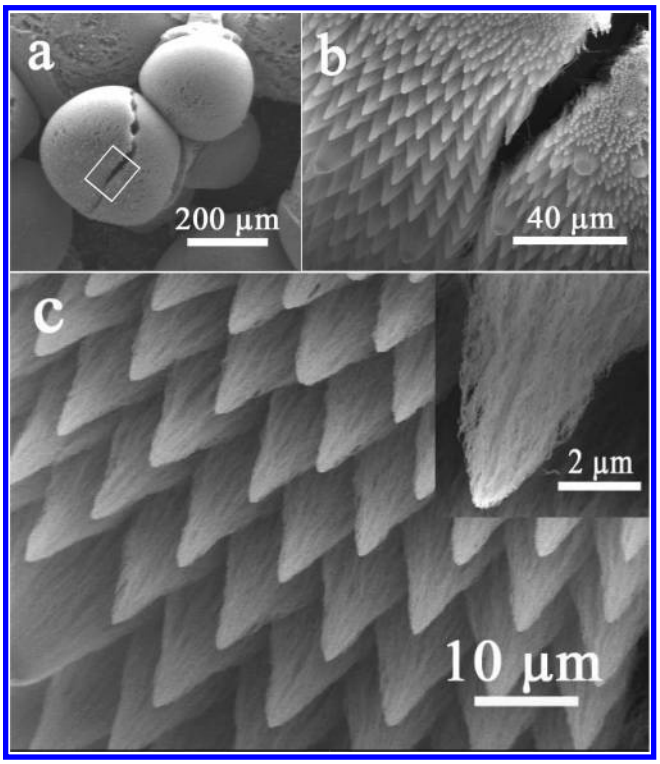


**Figure 2.** (a) SEM image of type II hollow spherical architectures on the Si wafer. (b) Enlarged SEM image from the broken area marked in the white pane in a. (c) High-magnified SEM image of the outer surface of type II hollow spherical architecture.

smooth. An enlarged SEM image (Figure 2b) of the outer surface of the sphere (marked in white pane in Figure 2a) shows that bundles of NWs directly assemble themselves into the hollow spheres. Careful observation (Figure 2c) on the external

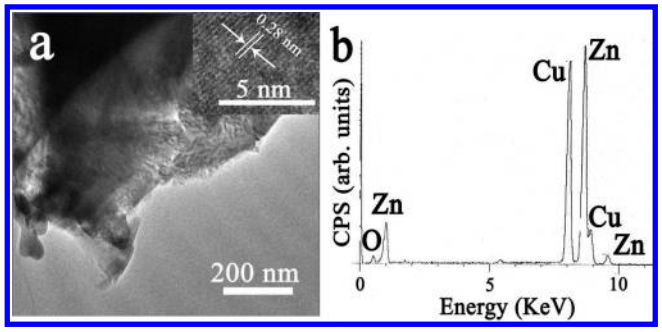


**Figure 3.** (a) TEM image of the ZnO spherical outer crust of type I architecture, and the inset is the HRTEM image. (b) EDS spectrum from the crust.

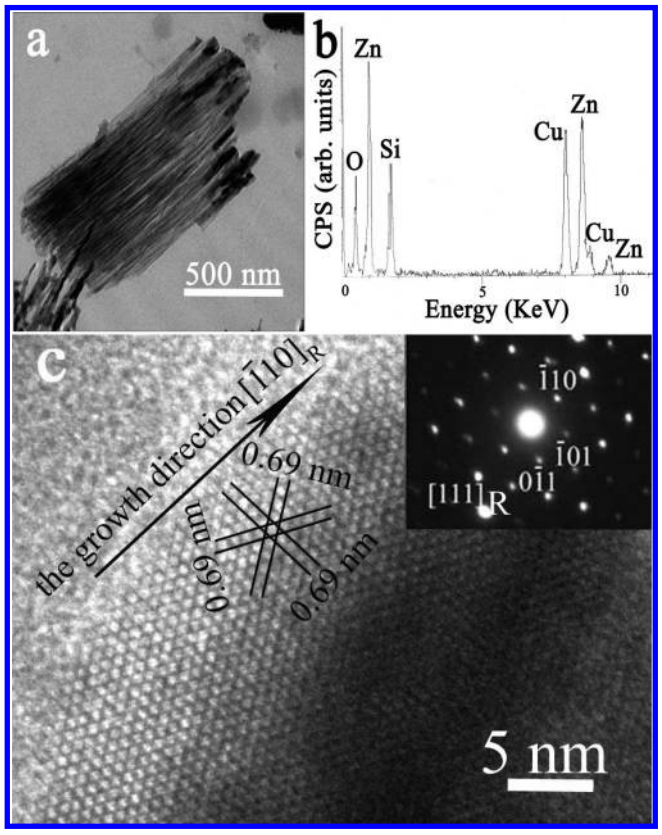


**Figure 4.** (a) TEM image of bundles of $Zn_2SiO_4$ NWs. (b) EDS spectrum from the NWs. (c) HRTEM image of a single $Zn_2SiO_4$ NW and the corresponding SAED pattern (inset).

surface reveals that well-aligned NWs grow outward radially, with their tips forming numerous novel architectures looking like closely packed Chinese writing brush heads and with each "brush head" composed of well-aligned NWs (the inset in Figure 2c).

Figure 3a is a TEM image of the outer crust of the hollow spherical architecture with smooth surface (type I) after being sonicated. EDS (Figure 3b) recorded from the outer crust indicates the presence of Zn and O, with an atomic ratio about 1:1. HRTEM image (the inset in Figure 3a) reveals that the crust is partially crystallized, with a lattice spacing about 0.28 nm, corresponding to the (100) interplanar distance of hexagonal ZnO. Figure 4a depicts TEM image of a pack of the NWs from the spherical shell after being sonicated. The corresponding EDS spectrum (Figure 4b) shows that the NWs are composed of Zn, Si, and O, with an atomic ratio of about 2:1:4. The HRTEM image (Figure 4c) demonstrates that the NWs are well-crystallized. The measured lattice spacing of 0.69 nm is consistent with the *d* value of $\langle \bar{1}10 \rangle_R$ planes of $Zn_2SiO_4$.

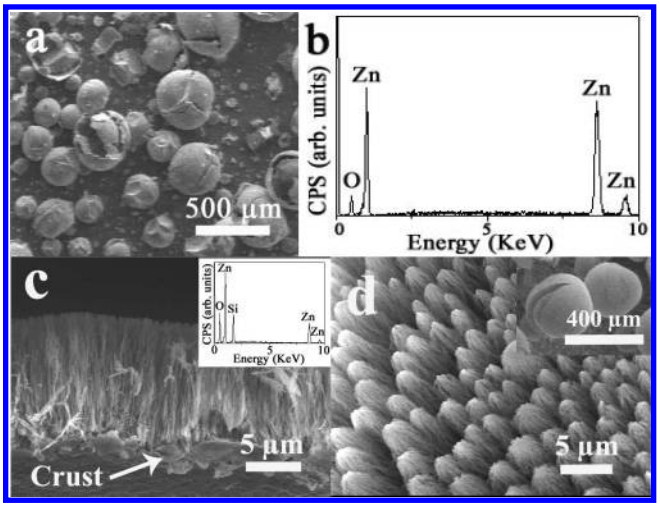


**Figure 5.** (a) Overview SEM image of the hollow spherical architectures, obtained by using $(MgCO_3)_4 \cdot Mg(OH)_2 \cdot 5H_2O$ in the mixture. (b) EDS spectrum of the ZnO spherical outer nanocrust. (c) Side view SEM image of the shell of type I hollow spherical architecture, and the inset is the EDS spectrum of the $Zn_2SiO_4$ NWs. (d) Enlarged SEM image of the outer surface of type II hollow spheres (the inset).

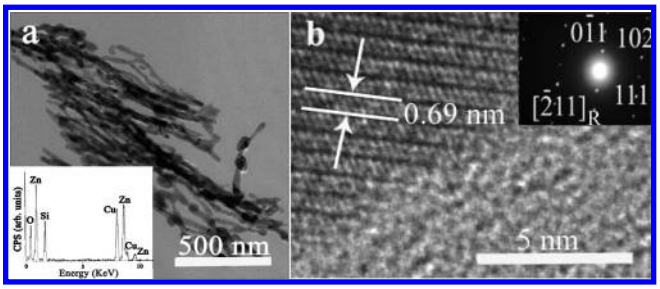


**Figure 6.** (a) TEM image of a bundle of $Zn_2SiO_4$ NWs, and the inset is the EDS spectrum from the NWs. (b) HRTEM image of a single $Zn_2SiO_4$ NW, and the corresponding SAED pattern in the inset.

Selected area electron diffraction (SAED) pattern on the upper-right inset is taken along the$[111]_R$ zone axis. Taken together, the NWs are $Zn_2SiO_4$ with an orientation along $[\bar{1}10]_R$ direction.

**3.2. Hollow Microspherical Architectures Obtained by Using Other Carbonates in the Raw Materials.** When $(MgCO_3)_4 \cdot Mg(OH)_2 \cdot 5H_2O$ was used in the mixture instead of $ZnCO_3 \cdot 2Zn(OH)_2 \cdot H_2O$, similar architectures have been obtained on the Si substrate. An overview SEM image (Figure 5a) of the products reveals very similar spherical architectures to those in Figure 1a. The spherical architectures are also hollow with diameters of about several hundreds of micrometers. Further observations reveal that there are also two types of hollow spheres, similar to those obtained from $ZnCO_3 \cdot 2Zn(OH)_2 \cdot H_2O$ in the raw materials. Side view SEM image (Figure 5c) of the shell from type I spherical architectures demonstrates that aligned NWs grow radially inward on the inner surface of the crust. EDS analysis on the outer crust shows chemical composition of ZnO (Figure 5b), and EDS spectrum (the inset in Figure 5c) taken from the NWs displays the chemical composition of $Zn_2SiO_4$. The enlarged image (Figure 5d) on the outer surface of type II sphere (the inset) shows that highly oriented NWs directly form themselves into the shell of the hollow spheres, being similar to those in Figure 2c. TEM image (Figure 6a) of the NWs reveals a bundle of highly aligned NWs, and the inset EDS spectrum further confirms that the chemical composition of the NWs is $Zn_2SiO_4$. HRTEM image (Figure 6b) of one NW reveals that the NW is single crystalline and free of defects. The lattice planes with spacing of 0.69 nm can be indexed to the $(0\bar{1}1)_R$ planes of $Zn_2SiO_4$. SAED pattern in the inset is taken

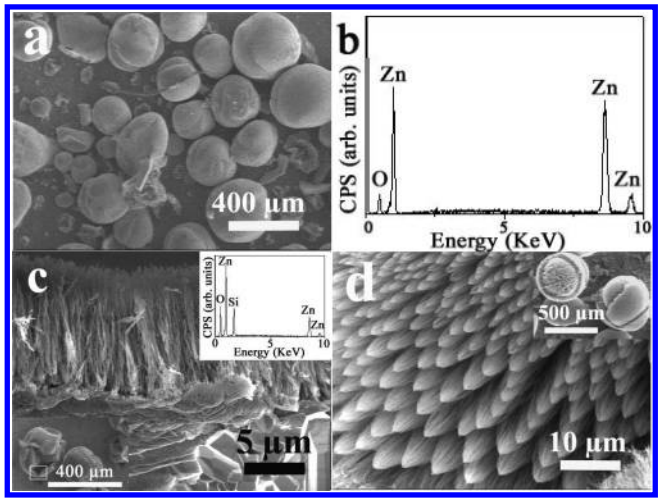


**Figure 7.** (a) Low-magnification SEM image of the hollow spherical architectures on the Si wafer, obtained by using $MnCO_3$ in the mixture. (b) Side view SEM image of the shell of type I hollow spherical architecture (lower-left inset), and the upper-right inset is the EDS spectrum of $Zn_2SiO_4$ NWs. (c) SEM image of the surface of type II hollow spherical architecture (the inset).

along the $[\bar{2}11]_R$ zone axis. When $MnCO_3$ was used in the mixture instead of $ZnCO_3{\cdot}2Zn(OH)_2{\cdot}H_2O$ or $(MgCO_3)_4{\cdot}Mg(OH)_2{\cdot}5H_2O$, the same spherical architectures (Figure 7a) also have been obtained similar to those shown in Figure 1a and Figure 5a. EDS spectrum (Figure 7) also reveals that the chemical composition of the spherical crust is ZnO. An enlarged side view SEM image (Figure 7c) of the shell from type I spherical architectures reveals that highly aligned NWs grow radially inward. EDS spectrum (the inset in Figure 7c) taken from the NWs also shows that the chemical composition of the NWs is $Zn_2SiO_4$. From a high-magnification SEM image (Figure 7d) of the external surface of type II hollow sphere (the inset), it can be seen that clumps of $Zn_2SiO_4$ NWs also looking like Chinese writing brush heads grow radially outward and directly form themselves into the shell of the hollow spheres.

**3.3. Growth Process of Hollow Microspherical Architectures.** On the basis of the above experiment results, we find that although $(MgCO_3)_4{\cdot}Mg(OH)_2{\cdot}5H_2O$ or $MnCO_3$ was used as raw materials, no Mg or Mn elements could be found in the final spherical outer crust and in the closely packed NWs. Also, if we only use Zn powder as the raw material with other experimental conditions being identical, no spherical architectures could be achieved on the Si wafer, indicating that $CO_2$ or $H_2O$ coming from the reaction of the raw materials plays an important role in the formation of hollow spherical architectures. Furthermore, if the Si wafer was replaced by quartz and sapphire substrates in the experiments, then only some crusts were formed on these substrates but without any NWs. Accordingly, the Si wafer is also crucial in the formation of spherical architectures. Then, possible formation processes of the two types of hollow spherical architectures are proposed, which is similar to the formation of ZnO[9] or CuO[5] "dandelions" through a growth-assembly process. First, Zn atoms are generated from Zn powders when the raw materials are heated in the beginning. The generated Zn atoms are transported to the lower temperature region by the carrier Ar gas and deposits on the Si wafer to form spherical Zn particles similar to those reported previously,[7,8] as shown in Figure 8a. These Zn spheres will be used as nuclear site or "template" for the formation of hollow spherical architectures, being similar to the formation of ZnO spheres on Zn particles reported previously.[7,8,17] Meanwhile, the carbonate in the mixture will be decomposed. For example, if

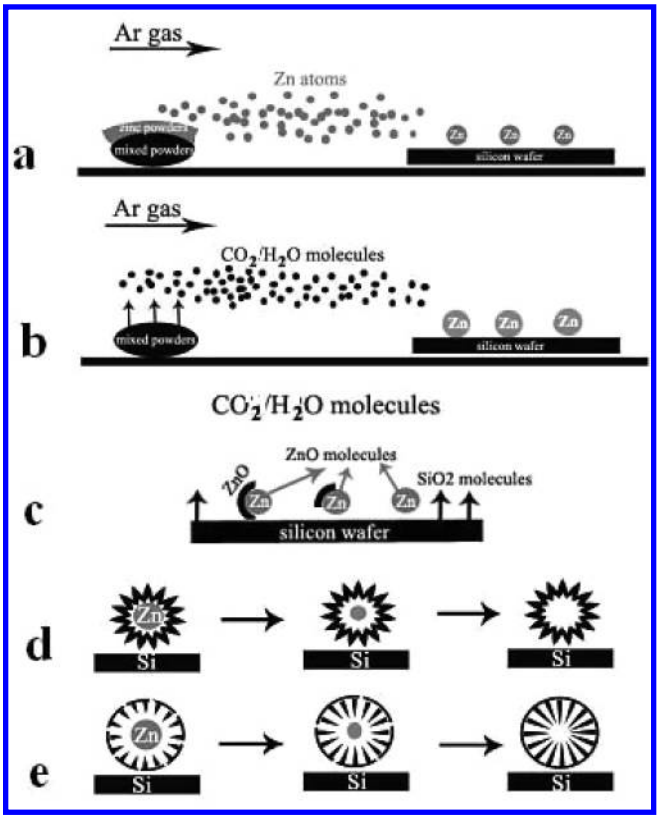


**Figure 8.** Schematic diagram illustration for the formation processes of the two types of hollow spherical architectures.

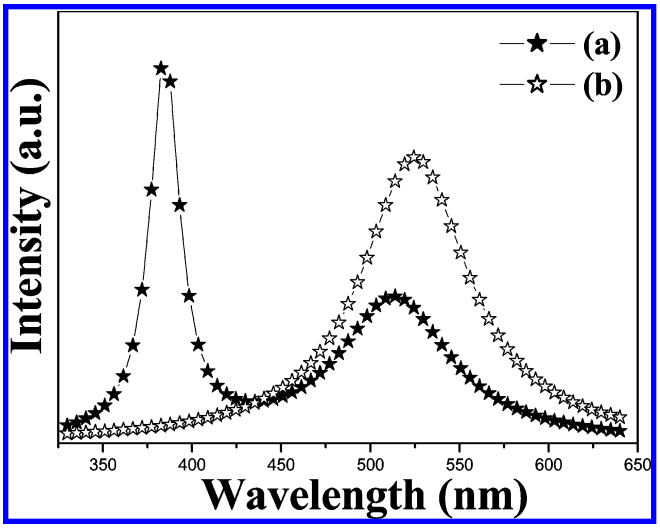


**Figure 9.** PL spectra taken from (a) the outer spherical nanocrust of ZnO and (b) the $Zn_2SiO_4$ NWs with an excitation wavelength of 325 nm at room temperature.

$ZnCO_3{\cdot}2Zn(OH)_2{\cdot}H_2O$ is used in the mixture, it will be decomposed into ZnO, $CO_2$, and $H_2O$.[18] Meanwhile, graphite will react with the decomposed ZnO and the residual $O_2$ in the tube, forming $CO_2$.[13] Similarly, if $(MgCO_3)_4{\cdot}Mg(OH)_2{\cdot}5H_2O$ or $MnCO_3$ is used in the raw materials instead of $ZnCO_3{\cdot}2Zn(OH)_2{\cdot}H_2O$, they will be decomposed into $CO_2$, $H_2O$, and MgO or manganese oxide.[19,20] The obtained oxides would further react with graphite to form $CO_2$. Therefore, with the increase of heating time at 1000 °C, there exists a large quantity of $CO_2$ and $H_2O$, which would be transported to the lower temperature region, as displayed in Figure 8b. Subsequently, the $CO_2$ and $H_2O$ vapors reach the Si wafer covered with spherical particles of liquid Zn and then react with both the Zn particles and the Si wafer. It has been reported that $CO_2$[21] and $H_2O$[22] could react

with Si atoms evaporated from the Si wafer to form $SiO_x$ molecules.[23] In the meantime, Zn particles react with $CO_2$, $H_2O$ vapor, and residual $O_2$[5,6,17,24] to form ZnO molecules, some of which will directly form a layer of ZnO on some Zn particles, as depicted in Figure 8c. Then, with further increase of the reaction time, the $SiO_x$ molecules would react with ZnO molecules vaporized from the surface of Zn particles to form $Zn_2SiO_4$.[25,26] If the unoxidized Zn particles are used as template (Figure 8d), the $Zn_2SiO_4$ molecules will deposit on the bare Zn particles and will grow into closely packed and radially well-aligned NWs covering the Zn particles, being similar to the formation of ZnO NWs on ZnO hollow spheres.[7] In the meantime, when the furnace is heated to 1000 °C, and the temperature of the substrate is around 900 °C, the Zn particles inside the aligned NWs will be easily sublimated. With the increase of reaction time, the Zn sphere inside the closely packed and radially well-aligned $Zn_2SiO_4$ NWs will be completely sublimated, and then type II hollow spheres could be formed on the Si wafer, as shown in Figure 8d. Bundles of $Zn_2SiO_4$ NWs looking like Chinese writing brush heads are probably formed through oriented attachment.[27] The formation of type I hollow spheres is similar to that of type II, except that the inner surface of the ZnO shell is used as the template or nuclear site for the $Zn_2SiO_4$ NWs (Figure 8e). As for the interim Zn−ZnO core−shell structures formed in the early age of the experiment, the ZnO shell may not completely cover the Zn particles, or there may be a crevice in the ZnO shell. As the inside Zn particles are sublimated, there will be empty space between the Zn particle and the ZnO shell. The $CO_2$, $H_2O$ vapor, and the residual $O_2$ in the furnace may enter the empty space between the Zn particle and the ZnO shell and may react with Zn vapor to form ZnO molecules, some of which will deposit on the inner surface of ZnO crust. The formed $SiO_x$ molecules can also enter the empty space between ZnO layer and Zn particle from the crevice and then can react with ZnO molecules to form $Zn_2SiO_4$ NWs, which grow inward from the inner surface of the ZnO shell and form themselves into closed packed and radially well-aligned NW architectures. After the Zn particles are sublimated completely, type I hollow spheres will be formed, as shown schematically in Figure 8e.

**3.4. Photoluminescence Properties of Hollow Microspherical Architectures.** Room-temperature PL spectrum (Figure 9a) taken only from the ZnO spherical outer crust displays two emission bands. A strong ultraviolet emission at about 380 nm attributed to the exciton-related emission near the band edge,[14] and a broad green emission centered at about 510 nm is associated with the singly ionized oxygen vacancies and interstitials of zinc and oxygen.[28] The PL spectrum (Figure 9b) from the closely packed and radially well-aligned $Zn_2SiO_4$ NWs only reveals a green emission at about 520 nm, being similar to that of bulk crystal $Zn_2SiO_4$.[25,26,29]

## 4. Conclusion

In summary, a simple thermal evaporation and condensation process has been demonstrated for the hollow spherical architectures consisting of closely packed and radially well-aligned $Zn_2SiO_4$ NWs with and without a thin layer of ZnO spherical outer crust. We find that similar spherical architectures can be achieved on the Si wafer by using a mixture of any of three carbonates ($ZnCO_3 \cdot 2Zn(OH)_2 \cdot H_2O$, $(MgCO_3)_4 \cdot Mg(OH)_2 \cdot 5H_2O$, and $MnCO_3$) in the raw materials, providing a possible method to synthesize similar architectures of other materials. The major hollow spheres consist of closely packed and well-aligned $Zn_2SiO_4$ NWs growing radially inward from the inner surface of ZnO spherical outer crust. The minor ones are composed of highly oriented $Zn_2SiO_4$ NWs growing radially outward, with their tips forming numerous architectures looking like Chinese writing brush heads. The thin layer of ZnO spherical outer crust has a strong UV emission at about 390 nm and a green emission at about 510 nm, while the $Zn_2SiO_4$ NWs have a broad green emission centered at about 520 nm. The novel hollow spherical architectures may have potentials in future optoelectronic devices.

**Acknowledgment.** This work was financially supported by the National Science Fund for Distinguished Young Scholars (Grant No.50525207), the Natural Science Foundation of China (Grant No.10374092), the Knowledge Innovation Program of the Chinese Academy of Sciences (Grant No. KJCX2-SW-W31), and the National Major Project of Fundamental Research: Nanomaterials and Nanostructures (Grant No. 2005CB623603).

## References and Notes

(1) Shi, H. T.; Qi, L. M.; Ma, J. M.; Cheng, H. M.; Zhu, B. Y. *Adv. Mater.* **2003**, *15*, 1647.
(2) He, T.; Chen, D. R.; Jiao, X. L.; Xu, Y. Y.; Gu, Y. X. *Langmuir* **2004**, *20*, 8404.
(3) Feng, X. J.; Zhai, J.; Jiang, L. *Angew. Chem., Int. Ed.* **2005**, *44*, 5115.
(4) Naik, S. P.; Chiang, A. S. T.; Thompson, R. W.; Huang, F. C. *Chem. Mater.* **2003**, *15*, 787.
(5) Liu, B.; Zeng, H. C. *J. Am. Chem. Soc.* **2004**, *126*, 8124.
(6) Goldberger, J.; He, R. R.; Zhang, Y. F.; Lee, S.; Yan, H. Q.; Choi, H. J.; Yang, P. D. *Nature* **2003**, *422*, 599.
(7) Shen, G. Z.; Bando, Y.; Lee, C. J. *J. Phys. Chem. B* **2005**, *109*, 10578.
(8) Gao, P. X.; Wang, Z. L. *J. Am. Chem. Soc.* **2003**, *125*, 11299.
(9) Liu, B.; Zeng, H. C. *J. Am. Chem. Soc.* **2004**, *126*, 16744.
(10) Mo, M.; Yu, J. C.; Zhang, L. S.; Li, K. A. *Adv. Mater.* **2005**, *17*, 756.
(11) Park, S.; Lim, J. H.; Chung, S. W.; Mirkin, C. A. *Science* **2004**, *303*, 348.
(12) O'Dwyer, C.; Navas, D.; Lavayen, V.; Benavente, E.; Santa, Ana, M. A.; Gonza'lez, G.; Newcomb, S. B.; Sotomayor Torres, C. M. *Chem. Mater.* **2006**, *18*, 3016.
(13) Gao, P. X.; Lao, C. S.; Ding, Y.; Wang, Z. L. *Adv. Funct. Mater.* **2005**, *16*, 53.
(14) Huang, M. H.; Mao, S.; Feick, H.; Yan, H. Q.; Wu, Y. Y.; Kind, H.; Weber, E.; Russo, R.; Yang, P. D. *Science* **2001**, *292*, 1897.
(15) Yang, L. W.; Wu, X. L.; Huang, G. S.; Qiu, T.; Yang, Y. M.; Siu, G. G. *Appl. Phys. A* **2005**, *81*, 929.
(16) Xiong, L. M.; Shi, J. L.; Gu, J. L.; Li, L.; Huang, W. M.; Gao, J. H.; Ruan, M. L. *J. Phys. Chem. B* **2005**, *109*, 731.
(17) Fan, H. J.; Scholz, R.; Kolb, F. M.; Zacharias, M.; Gosele, U. *Solid State Commun.* **2004**, *130*, 517.
(18) Kanari, N.; Mishra, D.; Gaballah, I.; Dupré, B. *Thermochim. Acta* **2004**, *410*, 93.
(19) Khan, N.; Dollimore, D.; Alexander, K.; Wilburn, F. W. *Thermochim. Acta* **2001**, *367−368*, 321.
(20) Shaheen, W. M.; Selim, M. M. *Thermochim. Acta* **1998**, *322*, 117.
(21) Li, S. H.; Zhu, X. F.; Zhao, Y. P. *J. Phys. Chem. B* **2004**, *108*, 17032.
(22) Zheng, B.; Wu, Y. Y.; Yang, P. D.; Liu, J. *Adv. Mater.* **2002**, *14* 122.
(23) Wei, Q.; Meng, G. W.; An, X. H.; Hao, Y. F.; Zhang, L. D. *Solid State Commun.* **2006**, *138*, 325.
(24) Yu, W. D.; Li, X. M.; Gao, X. D. *Cryst. Growth Des.* **2005**, *5* 151.
(25) Xu, C.; Chun, J.; Rho, K.; Kim, D. E. *Nanotechnology* **2005**, *16*, 2808.
(26) Wang, X. D.; Summers, C. J.; Wang, Z. L. *Adv. Mater.* **2004**, *16*, 1215.
(27) Banfield, J. F.; Welch, S. A.; Zhang, H. Z.; Ebert, T. T.; Penn, R. L. *Science* **2000**, *289*, 751.
(28) Vanheusden, K.; Warren, W. L.; Seager, C. H.; Tallant, D. R.; Voigt, J. A.; Gnade, B. E. *J. Appl. Phys.* **1996**, *79*, 7983.
(29) Feng, X.; Yuan, X. L.; Sekiguchi, T.; Lin, W. Z.; Kang, J. Y. *J. Phys. Chem. B* **2005**, *109*, 15786.